Journal of Coordination Chemistry

ISSN: 0095-8972 (Print) 1029-0389 (Online) Journal homepage: http://www.tandfonline.com/loi/gcoo20

Graphic data analysis and complex formation curves as modeling and optimization tools for characterization of Cu–(buffer)$_x$–(OH)$_y$ systems involving BTP or BES in aqueous solution

S. Maryam Sadeghi, Carlos M.H. Ferreira, Sarah Vandenbogaerde & Helena M.V.M. Soares

To cite this article: S. Maryam Sadeghi, Carlos M.H. Ferreira, Sarah Vandenbogaerde & Helena M.V.M. Soares (2015) Graphic data analysis and complex formation curves as modeling and optimization tools for characterization of Cu–(buffer)$_x$–(OH)$_y$ systems involving BTP or BES in aqueous solution, Journal of Coordination Chemistry, 68:5, 777-793, DOI: 10.1080/00958972.2014.1000317

To link to this article: http://dx.doi.org/10.1080/00958972.2014.1000317

Accepted author version posted online: 22 Dec 2014.
Published online: 27 Jan 2015.

Journal of Coordination Chemistry, 2015
Vol. 68, No. 5, 777–793, http://dx.doi.org/10.1080/00958972.2014.1000317

Graphic data analysis and complex formation curves as modeling and optimization tools for characterization of Cu–(buffer)$_x$–(OH)$_y$ systems involving BTP or BES in aqueous solution

S. MARYAM SADEGHI†, CARLOS M.H. FERREIRA†, SARAH VANDENBOGAERDE†‡ and HELENA M.V.M. SOARES†*

†Faculty of Engineering, REQUIMTE–Department of Chemical Engineering, University of Porto, Porto, Portugal
‡Industrial Engineering, Department Biochemistry-Microbiology, KaHo St.-Lieven, Gent, Belgium

(*Received 11 March 2014; accepted 4 December 2014*)

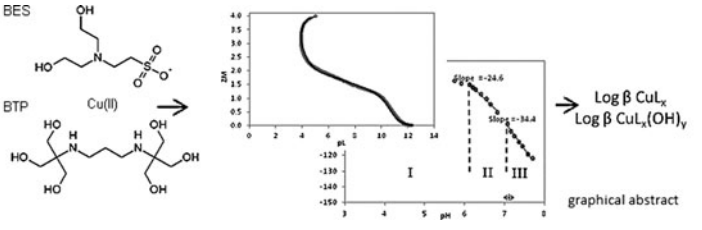

Bis-tris propane or 1,3-bis(tris(hydroxymethyl)methylamino)propane (BTP) and N,N-bis(2-hydroxyethyl)-2-aminoethanesulfonic acid (BES) are pH buffers which have been used in biological experiments. To characterize BTP and BES complexation properties with Cu(II), glass electrode potentiometry and direct current polarography were conducted using total ligand to total copper concentration ratios of different orders of magnitude and pH values at 25 °C and 0.1 M KNO_3 ionic strength. The graphic analysis is a very powerful tool in the prediction and refinement operations of both systems. For the Cu-BTP system, six species were found to describe totally the system, CuL, CuL(OH), CuL(OH)$_2$, CuL$_2$, CuL$_2$(OH), and CuL$_2$(OH)$_2$, with respective stability constants determined as 10.7 ± 0.1, 19.4 ± 0.4, 24.3 ± 0.2, 18.8 ± 0.1, 24.7 ± 0.2, and 29.8 ± 0.2. CuL$_2$, CuL$_2$(OH), and CuL$_2$(OH)$_2$ were described for the first time. In the case of the Cu-BES system, complexation behavior was described by the model constituted by CuL, CuL(OH), and CuL(OH)$_2$, the latter two described for the first time, with respective stability constants determined as 3.24 ± 0.08, 10.9 ± 0.2, and 16.0 ± 0.3, respectively. UV–vis results allowed us to establish coordination modes for the Cu-BTP and Cu-BES complexes.

Keywords: Metal speciation; Biological buffer; Stability constants; Potentiometry; Polarography

1. Introduction

In biological experimental studies, it is often desirable to maintain a stable pH due to the effects of hydrogen concentration on biological variables such as the rate of enzymatic

*Corresponding author. Email: hsoares@fe.up.pt

reactions, stability of biological molecules, the overall fitness of the cell, and the efficiency of several chemical reactions within the cell. For this purpose, biological buffers are usually used; Good and co-workers have developed a series of zwitterionic buffers containing amines, hydroxyl groups, and N-substituted amino sulfonic acid groups, usually known as Good's buffers [1–3]. Many experiments that require pH control also include metal ions; so, one of Good's requirements for a good biological buffer is that it does not complex metal ions or if it complexes, metal stability constants must be known and considered [1].

The 1,3-bis(tris(hydroxymethyl)methylamino)propane (BTP) is a biological zwitterionic buffer available from Sigma–Aldrich. It has two secondary amines, which are responsible for its two protonation constants, as shown in figure 1. The buffering pH range of BTP ($6.30 < pH < 9.50$) is of interest in plant physiology [4], chromatography [5, 6], and biotechnology [7]. The structure of BTP suggests that it should be a strong complexing agent. In fact, previous studies have shown that BTP forms strong complexes with Cd(II), Co(II), Ni (II), Pb(II), and Zn(II) [8, 9], and Cu(II) ions [10]. The model described in the literature for the Cu-BTP system is comprised of three species [CuL, CuL(OH), and $CuL(OH)_2$]. However, the analysis of the structure of BTP (figure 1) together with the models described for other divalent metal-BTP systems [8, 9], and the one described in the literature for Cu-BTP system [10] support the idea that this system is not properly described by the current model.

N,N-bis(2-hydroxyethyl)-2-aminoethanesulfonic acid (BES) is one of the buffers originally proposed by Good *et al*. [1]. BES is a zwitterionic buffer which contains a tertiary amine as shown in figure 1. Its buffering pH range ($6.40 < pH < 7.80$) makes BES suitable for biological studies. Recent studies describe the use of BES for this purpose [11–15]. There is evidence that BES complexes with Cu(II) [16]; however, this study only describes formation of CuL species. The comparative analysis between the structure of BES with other biological buffers containing similar structures, such as *N*,*N*-bis(2-hydroxyethyl) amino]-2-hydroxypropanesulfonic acid (DIPSO) [17], N-(2-acetamido)-2-aminoethanesulfonic acid (ACES) [18], and triethanolamine (TEA) [19], for which several $CuL_x(OH)_y$ species are described raises the hypothesis that Cu-BES system is not well characterized in the whole buffering pH range.

Although both Cu-BES and Cu-BTP systems have been already studied, our analyses suggest that the models described in the literature do not describe properly the complexation behavior between Cu(II) and these buffers. Considering the importance of knowing the

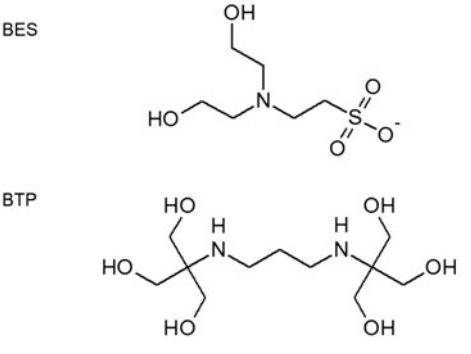

Figure 1. Structure of N,N-bis (2-hydroxyethyl)-2-amino ethane sulfonic acid (BES) and 1,3-bis(tris(hydroxymethyl)methylamino)propane (BTP).

correct speciation of Cu(II), when BTP or BES buffers are used, we decided to revisit and reevaluate complexation properties of these two Cu(II)-buffer systems. For this purpose, stability constant values for all Cu(II)-buffer species formed for each Cu-buffer system were determined by glass electrode potentiometry (GEP) and direct current polarography (DCP), using total ligand to total copper concentration ($[L_T] : [Cu_T]$) ratios of various orders of magnitude and various pH values at 25 °C and 0.1 M KNO_3 ionic strength. Additionally, spectroscopic properties of Cu(II) complexes were characterized by means of UV–visible (UV–vis) spectroscopy.

2. Experimental

2.1. *Material and reagents*

Stock standard solution of Cu(II) with a concentration of 1000 mg L^{-1} was obtained from Merck. The buffers, BTP (99%) and BES (99%), were purchased from Sigma Aldrich (St. Louis, MO, USA) and used as received. Potassium nitrate was used to set the ionic strength of solutions to 0.1 M for GEP and DCP. A 0.1 M KOH was standardized with potassium hydrogen phthalate by potentiometric titration as previously reported [20]. High purity nitrogen was used for deaeration of the sample solutions to remove the dissolved oxygen and carbon dioxide. Additional information about the remaining materials was described previously [20].

2.2. *Apparatus*

All the potentiometric and polarographic experiments were performed in a Metrohm (Herisau, Switzerland) jacketed glass vessel and thermostated at 25.0 ± 0.1 °C in water bath with magnetic stirrer.

The potentiometric titrations were carried out using a PC-controlled system assembled with a Crison MicropH 2002 meter, a Crison MicroBU 2030 microburette, a Philips GAH 110 glass electrode, and an Orion 90-02-00 (double junction) reference electrode with the outer chamber filled with 0.1 M potassium nitrate. Automatic acquisition of data was done using a home-made program, COPOTISY.

All polarographic measurements were performed with a Model 663 VA stand (Metrohm) with a dropping mercury electrode, as working electrode, a silver/silver chloride (3 M KCl) and a glassy carbon, as reference and counter electrodes, respectively; all electrodes were obtained from Metrohm, as previously described [20]. The VA stand was coupled to a micro-Autolab system (Eco Chemie, Utrecht, The Netherlands) controlled by a personal computer. The pH measurements were carried out with a GPL22 meter (Crison, Barcelona, Spain) with a sensitivity of ±0.1 mV (±0.001 pH units) with a combined silver/silver chloride reference electrode/glass electrode (Crison Switzerland).

2.3. *Procedure*

For all potentiometric and polarographic titrations, calibration of the glass electrode (pH measured as $-\text{Log}\,[H^+]$) was carried out using standardized solutions of nitric acid and potassium hydroxide following the procedure previously described by Machado *et al*. [20]. In short, rigorous volumes of standardized potassium hydroxide solution were added to a fixed volume

of standardized nitric acid solution, both with adjusted ionic strength of 0.1 M. From this, a potentiometric titration (potential *versus* pH plot) was drawn, and the E° and the response slope were obtained and used to calculate the pH in GEP and DCP experiments.

For the Cu-BTP system, only GEP was used in this work. Three different $[L_T]:[Cu_T]$ ratios were considered: 4, 2, and 1.05 with a copper concentration of 1×10^{-3} M. For each ratio, the number of independent solutions and titrations can be seen in table 1.

The Cu-BES system was studied by two independent techniques: GEP and DCP. For GEP experiments, two different $[L_T]:[Cu_T]$ ratios were used: 4 and 2 with a copper concentration of 1×10^{-3} M. For each ratio, the number of experiments performed is shown in table 1. For DCP experiments, a total of 4 titrations were carried out for different $[L_T]:[Cu_T]$ ($[L_T]:[Cu_T] = 50$, $[Cu_T] = 6 \times 10^{-5}$ M; $[L_T]:[Cu_T] = 100$, $[Cu_T] = 3 \times 10^{-5}$ M, and $[L_T]:[Cu_T] = 150$, $[Cu_T] = 2 \times 10^{-5}$ M) ratios as shown in table 1.

To evaluate the adsorption of BES on the surface of the working electrode, alternating current polarography (ACP) studies were conducted. AC polarograms for a BES concentration of 3×10^{-3} M were run without the metal ion using the experimental conditions described elsewhere [20]. The potential range used in the polarogram scans was 0.0 to −1.0 V *versus* Ag/AgCl(s), 3 M KCl, at two different pH values: 5.0, where most BES is in its HL form and 9.0, where BES is found mostly as L^-. AC polarograms were run at two different phase angles: 0° and 90°. For each condition tested, scans were made until at least three measurements were in agreement.

For all BTP and BES titrations, the pH range was from 2.5 to 11.0.

To investigate the complexes structures, UV–vis experiments were performed. Taking into account the information from the species distribution diagrams, sample solutions were prepared at the pH where the maximum quantity of a given species is predicted to exist. Therefore, for Cu-BTP system, six solutions, one for each species in study, were prepared at pH 6.7, 8.2, and 11 for $[L_T]:[Cu_T] = 1.05$ (corresponding to CuL, CuL(OH), and $CuL(OH)_2$, respectively) and pH 4.6, 6.9, and 11 for $[L_T]:[Cu_T] = 2$ (corresponding to CuL_2, CuL_2OH, and $CuL_2(OH)_2$, respectively). For Cu-BES system, due to precipitation, only solutions at pH 4, 5.6, and 6.1 were prepared for $[L_T]:[Cu_T] = 2$, corresponding to free metal, CuL and CuL(OH), respectively. A blank and metal only solutions were also prepared and read.

2.4. *Data treatment*

The program Equilibrium Simulation for Titration Analysis (ESTA) [21] was used for simulation and optimization procedures of potentiometric data. ESTA imposes the conditions of

Table 1. Number of independent solutions and total number of titrations used for each total ligand to total metal concentration ratio for Cu(II)-BTP and Cu(II)-BES systems.

Buffer	$[L_T]:[Cu_T]$	Number of solutions	Number of titrations	pH Range
BTP	4	2	3	2.5–11
	2	2	3	2.5–11
	1.05	2	4	2.5–11
BES	4	2	4	2.5–9
	2	1	2	2.5–9
	50	1	1	2.5–10
	100	1	1	2.5–10
	150	2	2	2.5–10

mass balance by equating calculated total concentrations with analytical concentrations. This program uses two distinct functions: *Z*-bar(H) (Z_H) and *Z*-bar(M) (Z_M). The first function depends only on pH and is very effective to predict the number of protonation steps and determination of protonation constants. The second function can be described as the number of ligands bound per metal ion at a certain titration point, and this function is calculated for each datum point and is plotted against −log[L] to aid in the modeling procedures. During the refinement, the dissociation constant of water, the protonation constants for the ligands (BTP or BES), as well as all known formation constants for $Cu_x(OH)_y$ species were kept fixed (table 2).

In the ACP data treatment, for each experimental condition tested the variation of the capacitance as a function of the potential was calculated. Calculation of the capacitance–potential curves was done from the resulting current intensities, recorded as described above. The value of the capacitance (C) was calculated using the impedance measurement data by following the equation:

$$C = \frac{-1}{Z'' \times 2 \times \pi \times f} \tag{1}$$

where Z'' is an imaginary component related to impedance and f the frequency; for further detail, see Bard and Faulkner [22].

The refinement of the polarographic data was conducted using the methodology described by Cukrowski [23]. This methodology uses mass balance equations for labile (on the polarographic time scale) and reversible metal ligand systems when studied at fixed $[L_T] : [M_T]$ ratio and variable pH. Then, a comparative analysis of the experimental and calculated complex formation curves (ECFC and CCFC, respectively) is conducted to refine the models proposed.

3. Results and discussion

3.1. *Complexation studies for the Cu-BTP-OH system*

For Cu(II)-BTP, two different $[L_T] : [Cu_T]$ ratios were carried out in order to test the stability constants reported in previous work by Hong and Bai [10]. The titration plots, with pH as a function of a, where a value is the ratio of moles of base added per mole of ligand present, can be seen in figure 2(A) for BTP. By comparing titration plots for the same concentration of ligand (curve *a* with curve *b* and curve *c* with curve *d*), it is possible to have a first glance at the complexation behavior of the metal ligand system. If no complexation happens, the titration plots would overlap. This is not observed; in fact, for the curves, differences are visible from very early, indicating that complexation starts as early as pH 3.5. The behavior of the titration also points out that more than one complex is being formed throughout the titration. For ratio of 4, the experimental curve of Z_M can be seen in figure 3(A). By making a simulation for the model reported by Hong and Bai [10], calculated Z_M values were plotted against our experimental data [figure 3(A) and (B)]; it is clearly visible that the reported model does not reproduce properly the experimental values. Similar results were obtained for all titrations conducted with $[L_T] : [Cu_T]$ ratios 4 and 2. In fact, the Z_M function, calculated assuming the stability constant values reported by Hong and Bai [10],

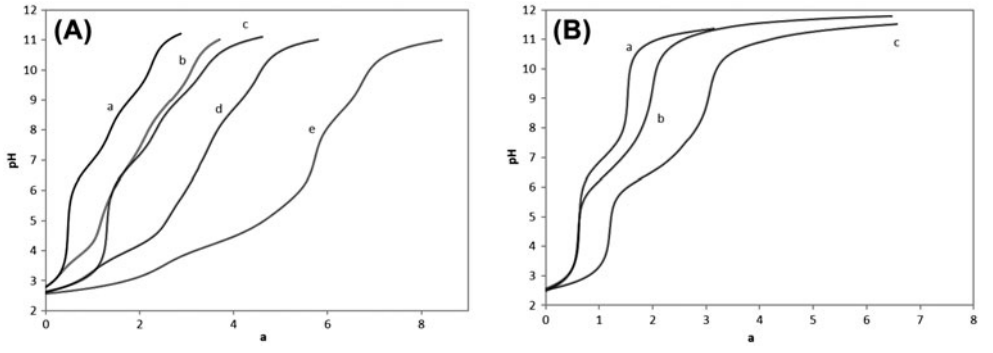

Figure 2. Potentiometric titration curves for (**A**) Cu(II)-BTP and (**B**) Cu(II)- BES systems with pH in function of number of moles of bases added per mole of ligand (a). For Cu(II)-BTP (**A**): curve *a*: $[L_T] = 4 \times 10^{-3}$ M; curve *b*: $[Cu_T] = 1.0 \times 10^{-3}$ M, $[L_T] : [Cu_T] = 4$; curve *c*: $[L_T] = 2 \times 10^{-3}$ M; curve *d*: $[Cu_T] = 1.0 \times 10^{-3}$ M, $[L_T] : [Cu_T] = 2$; curve *e*: $[Cu_T] = 1.0 \times 10^{-3}$ M, $[L_T] : [Cu_T] = 1.05$. For Cu(II)-BES (**B**): curve *a*: $[L_T] = 4 \times 10^{-3}$ M; curve *b*: $[Cu_T] = 1.0 \times 10^{-3}$ M, $[L_T] : [Cu_T] = 4$; curve *c*: $[Cu_T] = 1.0 \times 10^{-3}$ M, $[L_T] : [Cu_T] = 2$.

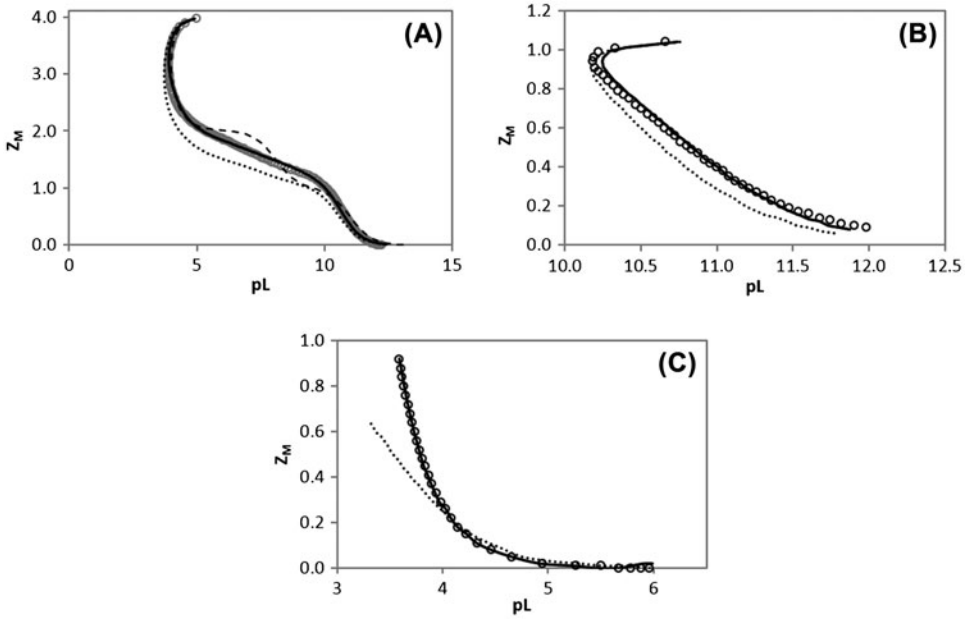

Figure 3. Z_M function for (**A, B**) Cu(II)-BTP and (**C**) Cu(II)-BES systems. (**A**) $[L_T] : [Cu_T] = 4$, (**B**) $[L_T] : [Cu_T] = 1.05$, and (**C**) $[L_T] : [Cu_T] = 4$, $[Cu_T] = 1.0 \times 10^{-3}$ M. Models and experimental conditions are described in tables 3 and 5 for BTP and BES, respectively. Model I (–), model II (—), proposed in this work, and previous one described in the literature (•••) *vs*. experimental data (○).

is below the experimental points, which corresponds to less complexation than really occurs. These observations were in agreement with our initial expectations that BTP seems to have strong complexing properties. Based on these results, we decided to perform an exhaustive complexation study of Cu(II) with BTP.

From the analysis of figure 3(A), it is possible to see an obvious increase to $Z_M = 1$ between pL 12 and 10 (pH 3.2–3.7), which clearly indicates formation of CuL in this pH range. From here, the Z_M values show a weaker increase to 2 (from pL 10 to 5) and then show signs of back-fanning. The growth of Z_M to 2 without back-fanning indicates formation of CuL_2 species. However, this growth does not present a characteristic growth pattern for CuL to CuL_2 transition (as shown in figure 3(A), model I); therefore, other species must be formed before or simultaneously with CuL_2, most likely $CuL(OH)_x$ as described by Hong and Bai [10]. Furthermore, after $Z_M = 2$, back-fanning is observed, which indicates the formation of hydroxide species at this point, presumably $CuL_2(OH)_x$ species.

According to this analysis, the best model to replicate the experimental data should be one containing CuL, $CuL(OH)_x$, CuL_2, and $CuL_2(OH)_x$ ($x = 1, 2$). Two models were tested and refined: model I including CuL, CuL_2, $CuL_2(OH)$, and $CuL_2(OH)_2$; and model II including CuL, CuL(OH), $CuL(OH)_2$, CuL_2, $CuL_2(OH)$, and $CuL_2(OH)_2$. The refined values for $[L_T] : [Cu_T]$ ratios 2 and 4 are presented in table 3. In figure 3(A), it is possible to see that model I (dashed line) fits poorly the experimental data, as it fails to fit the transition of $Z_M = 1$ to $Z_M = 2$. This was expected as stated earlier as the smoother transition from $Z_M = 1$ to $Z_M = 2$ seem to point out the formation of other species, namely $CuL(OH)_x$. Moreover, upon analyzing the values for the standard deviation and objective function (table 3), one can see that this model fits more poorly than model II. For higher pH (around 7, pL = 5), the model starts to fit more accurately, evidencing the formation of $CuL_2(OH)_x$ species. On the other hand, model II fits the model more accurately as shown in figure 3(A) and table 3. Inclusion of CuL(OH) greatly improves the model. However, $CuL(OH)_2$ was consistently rejected by the program, which may indicate that it is a minor species under the experimental conditions tested. Still, Hong and Bai included $CuL(OH)_2$ in their work, as a part of the model. In order to clarify this point, a third $[L_T] : [Cu_T]$ ratio of 1.05 was studied. At this ratio, CuL_2 and $CuL_2(OH)_x$ species should be present at very low quantities and thus can be disregarded; therefore, formation of $CuL(OH)_x$ species can be studied without interference of $CuL_2(OH)_x$ species. In this case, the purpose was to test the model CuL, CuL(OH), and $CuL(OH)_2$ (model III, table 3). Upon refinement, the model adjusted well to the experimental points [figure 3(B)]. The obtained values are not very different from the ones reported before by Hong and Bai (CuL = 10.57; CuL(OH) = 18.90, and $CuL(OH)_2$ = 24.27) [10]. Moreover, the magnitude of the refined stability constant values for CuL and CuL(OH) species are similar or close to the ones obtained for model II (table 3). A comparative analysis of the model refined by us and the one previously described in the literature can be seen in figure 3(B). Although, the previous model does not fit the experimental data, as expected by the differences in values obtained, the pattern followed by the model is similar with our experimental data. These results show that the species included in this model [CuL, CuL(OH), and $CuL(OH)_2$], already described in the literature, explains well the experimental conditions corresponding to $[L_T] : [Cu_T] = 1.05$, but not for higher $[L_T] : [Cu_T]$ ratios where other species [CuL_2 and $CuL_2(OH)_x$ species] are formed. Therefore, the final proposed model should include CuL, CuL(OH), $CuL(OH)_2$, CuL_2, CuL_2OH, and $CuL_2(OH)_2$ species and the values for the respective stability constants, refined simultaneously from all the titrations described in table 1, are found in table 4.

In order to test the model, a species distribution diagram (SDD) using the values of tables 2 and 4 for $[L_T] : [Cu_T] = 4$, $[Cu_T] = 1 \times 10^{-3}$ M was drawn [figure 4(A)]. From the analysis of SDD, it became obvious that CuL, CuL_2, $CuL_2(OH)$, and $CuL_2(OH)_2$ are major species in the system. Around pH 3.0, BTP starts to complex Cu(II) and a maximum amount (about 80%) of CuL is formed at pH 4.5, while a maximum amount (more

Table 2. Protonation constants for water, BTP, BES, and overall stability constants for Cu(II) complexes with OH^- at 25 °C.

	Equilibrium	Log β	μ (M L^{-1})	Ref.
Water	$H^+ + OH^- \rightleftarrows H_2O$	13.78	0.1	[19]
BTP	$BTP + H^+ \rightarrow HBTP^+$	9.07	0.1	[8]
	$BTP + 2H^+ \rightarrow H_2BTP^{2+}$	15.95	0.1	[8]
BES	$BES^- + H^+ \rightarrow HBES$	7.09	0.1	[16]
Copper	$Cu^{2+} + OH^- \rightleftarrows Cu(OH)^-$	6.1	0.1	[19]
	$Cu^{2+} + 2OH^- \rightleftarrows Cu(OH)_2$	11.8	0.1	[19]
	$2Cu^{2+} + 2OH^- \rightleftarrows Cu_2(OH)_2^{2+}$	16.8	0.1	[19]
	$3Cu^{2+} + 4OH^- \rightleftarrows Cu_3(OH)_4^{2+}$	33.5	0.1	[19]
	$Cu(OH)_2(s) \rightleftarrows Cu^{2+} + 2OH^-$	−18.5	0.7	[19]

Table 3. Stability constants (as log β) for Cu-BTP system, determined by GEP (one titration per ratio), at 25 °C and 0.1 M KNO_3 ionic strength.

$[L_T] : [Cu_T]$	4		2		1.05
$[Cu_T]$ (M)	1×10^{-3}		1×10^{-3}		1×10^{-3}
Complex	Model I	Model II	Model I	Model II	Model III
CuL	11.02 ± 0.04	10.76 ± 0.01	11.02 ± 0.06	10.48 ± 0.01	10.79 ± 0.01
CuL(OH)	NI	19.79 ± 0.02	NI	19.92 ± 0.01	18.99 ± 0.01
$CuL(OH)_2$	NI	R	NI	R	24.21 ± 0.02
CuL_2	19.12 ± 0.06	18.55 ± 0.01	19.82 ± 0.08	19.05 ± 0.01	NI
$CuL_2(OH)$	24.99 ± 0.08	24.59 ± 0.01	26.05 ± 0.09	25.08 ± 0.01	NI
$CuL_2(OH)_2$	30.15 ± 0.08	29.44 ± 0.02	31.45 ± 0.09	29.66 ± 0.02	NI
pH range	3.0–9.0	3.0–9.0	3.0–9.0	3.0–9.0	3.5–10.0
No of points	187	187	187	187	89
R factor	0.061	0.0095	0.081	0.026	0.0093

Notes: R – rejected, NI – not included.

Table 4. Overall stability constants (as log β) for the Cu-L-$(OH)_x$ system (L = BTP or BES), after combining all polarographic and potentiometric results, for ionic strength of 0.1 M at 25 °C.

Equilibrium	BTP[a]	BES[b]
Cu + L ⇌ CuL	10.7 ± 0.1	3.24 ± 0.08
Cu + L + OH ⇌ CuL(OH)	19.4 ± 0.4	10.9 ± 0.2
Cu + L + 2OH ⇌ $CuL(OH)_2$	24.3 ± 0.2	16.0 ± 0.3
Cu + 2L ⇌ CuL_2	18.8 ± 0.1	NI
Cu+ 2L + OH ⇌ $CuL_2(OH)$	24.7 ± 0.2	NI
Cu+ 2L + 2OH ⇌ $CuL_2(OH)_2$	29.8 ± 0.2	NI

[a]1191 experimental points from 10 independent titrations.
[b]281 experimental points from 10 independent titrations.
Notes: NI – not included.

than 80%) of CuL_2 occurs at pH 6.5, in conformity with the experimental data for Z_M. No precipitation is predicted, which corroborates the experimental observations. However, it should be noted that no formation of $CuL(OH)_2$ is predicted according to the SDD. This is due to the high $[L_T] : [Cu_T]$ ratio, where $CuL_2(OH)_x$ species are dominant and preferred over $CuL(OH)_x$ ones. This explains why it was not possible to refine $CuL(OH)_2$ for $[L_T]$:

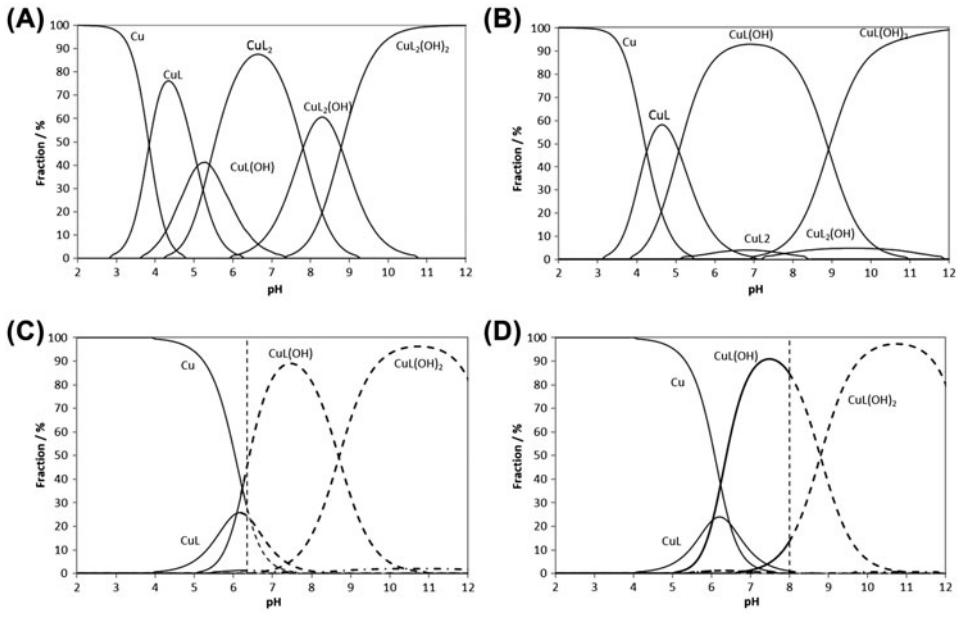

Figure 4. Species distribution diagrams for the final models, described in table 4, for (**A, B**) Cu(II)-BTP and (**C, D**) Cu(II)-BES systems. (**A**) $[L_T] : [Cu_T] = 4$, $[Cu_T] = 1 \times 10^{-3}$ M; (**B**) $[L_T] : [Cu_T] = 1.05$, $[Cu_T] = 1 \times 10^{-3}$ M; (**C**) $[L_T] : [Cu_T] = 4$, $[Cu_T] = 1 \times 10^{-3}$ M; (**D**) $[L_T] : [Cu_T] = 100$, $[Cu_T] = 3 \times 10^{-5}$ M. Dashed vertical lines represent precipitation events. Dashed curves after precipitation point represent hypothetical speciation. Lines with alternating dashing represent $Cu(OH)_x$ species. For sake of simplicity, charges were omitted.

$[Cu_T]$ ratios 4 and 2. Additionally, a SDD was also generated for $[L_T] : [Cu_T] = 1.05$, $[Cu_T] = 1 \times 10^{-3}$ M [figure 4(B)]. In this case, CuL(OH) and $CuL(OH)_2$ are the major species in the system, and the species formation patterns are in agreement with the experimental data seen in figure 3(B), where it is possible to see an increase of Z_M up to 1, related to CuL formation and then back-fanning, which is related to the formation of CuL(OH) and $CuL(OH)_2$.

3.2. *Complexation studies for the Cu-BES-OH system*

For the Cu(II)-BES system, two different $[L_T] : [Cu_T]$ ratios were performed using GEP for testing the stability constants reported in previous work [16]. In the titration plots for BES, figure 2(B), by comparing titration plots for ligand alone (curve a) and ligand at the same concentration with metal (curve b), it is possible to see that complexation starts at pH 5.5. The behavior of the titration plots also points out that more than one complex should be formed throughout the titration, since the shape of the curves of the metal-free ligand and of the ligand with metal are substantially different. Figure 3(C) shows the experimental values of Z_M for ratio 4. When using the model described in the literature [16], it is evident that this model does not explain the experimental data [figure 3(C)]. This test was carried out for all titrations and the same conclusion was obtained : Although the previous model adjusts well the experimental data until pH 5.5 (pL values >4), due to the formation of CuL, experimental data presented in figure 3(C) clearly evidence signs of back-fanning,

indicative of the formation of hydroxide species. These results indicate that the model described in the literature containing only CuL is not suitable to model the Cu-BES system in the pH buffering range. The best model to explain the experimental data would be one comprising CuL and $CuL(OH)_x$ species. Due to the occurrence of precipitation at pH 6.5, with both $[L_T]:[Cu_T]$ ratios, refinement operations could only be done below this pH. Therefore, only CuL and CuL(OH) were determined (table 5, model I). From these results, full characterization of BES complexation ability in its entire pH buffering range was not achieved. Therefore, further studies are needed in order to expand the pH range to higher values and thus, to investigate other species.

Considering that GEP was not able to define properly the Cu-BES system, we decided to study it by performing DCP titrations. This technique uses higher $[L_T]:[Cu_T]$ ratios with lower metal concentrations; under these experimental conditions, precipitation occurs at higher pH values, which allows studying the complexation of the metal–ligand systems at higher pH. For this purpose, four different DCP titrations were performed using different $[L_T]:[Cu_T]$ ratios ($[L_T]:[Cu_T]$ = 50, 100, and 155) in the pH range between 2.5 and 10.0. From analysis of the different DCP titrations, the Cu-BES system behaves as labile throughout the experiments. For all experiments, only one DC wave was observed, which moved to more cathodic values in the titration.

Since, metal stability constants determined by polarographic methods require the absence of adsorption of the ligand at the mercury surface electrode; previously, ACP experiments were performed in order to disclose the presence of such phenomena. The capacitance was calculated for each condition and compared with the electrolyte solution. Comparing the capacitance–potential curves recorded for the BES concentration of 3.0×10^{-3} M with those recorded in the presence of the electrolyte only (data not shown), no significant differences were observed. Based on these results, we can say that there is no significant adsorption at the mercury surface electrode for BES concentrations up to 3.0×10^{-3} M for the pH values tested.

For the DCP titrations, the shape and steepness of the waves, measured by the gamma coefficient, varied from the initial 1.0 at higher pH levels. In order to obtain accurate stability constants, refinement of the polarographic data requires that the curves be representative of a fully reversible electrochemical process. Therefore, a correction procedure, previously described [24], was applied. Briefly, this method corrects the semi-reversibility of the DCP data by fixing the gamma coefficient to 1.0, and then adjusting the limiting diffusion current and potential of the half height, $E_{1/2}$.

From analysis of the slope of the curve, acquired by plotting $E_{1/2}$ *versus* pH, it is possible to predict the species present at a given pH range. When a metal species is present, a slope of $m \times -59.16 \times n^{-1}$ should be observed in the plot (m and n stand for the number of protons and electrons involved in the electro-chemical reaction, respectively) [23]. As an example, analysis of the experimental data is presented for $[L_T]:[Cu_T]$ = 100. Figure 5(A) outlines three different regions. The first is at pH < 5.9, where no shift of potential was observed; this fact is indicative that no appreciable complexation takes place in this pH range. The second region goes from pH 5.9 to 6.6 where a slope of about −24.6 mV/pH units is visible. Considering that, at this pH the ligand is mostly HL, this slope may be related to the characteristic slope of −29.6 mV/pH found in the presence of CuL in the solution as described by the following reaction (charges were omitted for simplicity):

$$CuL + H + 2e \rightleftharpoons Cu(Hg) + HL \quad (2)$$

Table 5. Stability constants (as log β) for Cu-BES system determined by GEP and DCP at 25 °C and 0.1 M KNO_3 ionic strength.

	GEP		DCP					
$[L_T] : [Cu_T]$	2	4	50		100		150	
$[Cu_T]$ (M)	1×10^{-3}	1×10^{-3}	6×10^{-5}		3×10^{-5}		2×10^{-5}	
Complex	Model I	Model I	Model I	Model II	Model I	Model II	Model II	Model II
CuL	3.36 ± 0.04	3.27 ± 0.01	3.16 ± 0.05	3.22 ± 0.05	3.53 ± 0.04	3.23 ± 0.04	3.60 ± 0.05	3.29 ± 0.05
CuL(OH)	11.08 ± 0.04	11.06 ± 0.01	10.59 ± 0.02	10.51 ± 0.03	11.14 ± 0.02	10.74 ± 0.03	10.74 ± 0.03	10.67 ± 0.03
$CuL(OH)_2$	R	R	NI	15.9 ± 0.2	NI	16.3 ± 0.2	15.8 ± 0.4	15.7 ± 0.4
pH range	3.5–6.0	3.5–6.0	2.9–7.8	2.9–7.8	2.95–7.85	2.95–7.85	2.8–7.7	2.95–7.6
No of points	19	28	35	35	33	33	33	33
R factor	0.017	0.005	–	–	–	–	–	–
SD (mV)	–	–	0.39	0.26	0.53	0.40	1.72	0.85

Notes: R – rejected, NI – not included.

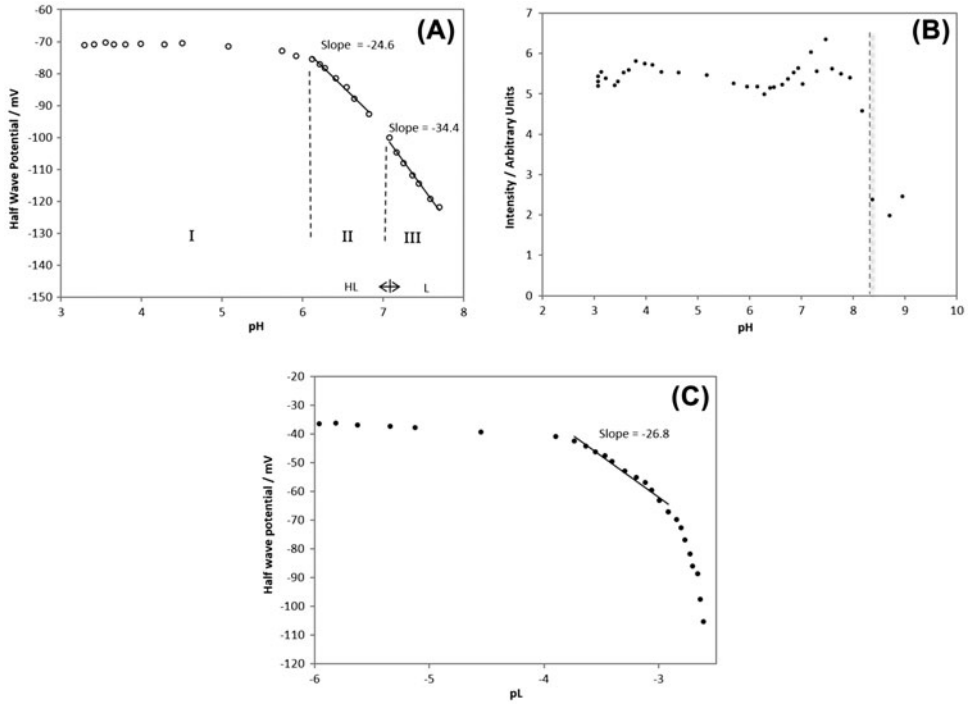

Figure 5. DCP experimental data for Cu(II)-BES system at 25 °C and 0.1 M KNO_3 ionic strength: Half-wave potential (**A**) and current intensity (**B**) in function of pH and half-wave potential in function of pL, (**C**).

This observation is in line with the model of GEP, which also predicts the formation of CuL at this pH range. The third region is found between pH 6.7 to about 7.8, where precipitation was observed under DCP conditions. To verify the maximum pH value where no precipitation was observed experimentally, we followed the normalized current [figure 5(B)]. From this figure, the marked drop of the intensity of the limiting current clearly suggests occurrence of precipitation for pH values higher than 8.2. Also, in this region, in particular for pH higher than 7.0, the ligand is mostly in its fully deprotonated form (L^-); therefore, the slope found in this region (about −34.4 mV/pH unit) may be related to the presence of a mixture of $CuL(OH)_y$ species. Under these experimental conditions, the presence of CuL(OH) gives a theoretical slope of about 29.6 mV per pH unit, as described by the following equation:

$$CuL_x(OH) + H + 2e \rightleftharpoons Cu(Hg) + xL + H_2O \quad (3)$$

However, as the experimental value found is higher (34.4 *versus* 29.6 mV per pH unit), other species, such as $CuL(OH)_2$, are probably present. If $CuL(OH)_2$ is formed, a slope of about −59.2 mV per pH unit would be observable. The intermediate value found can be due to a mixture of both species.

From analysis of the plot of $E_{1/2}$*versus* pL [figure 5(C)], only one slope of −26.8 mV per pL unit can be drawn, close to −29.6 mV per pL unit, which indicates the formation of CuL species. If CuL_2 was present, a slope of −59.2 mV per pL unit should be identified, which was not the case.

This graphic analysis indicates that the model that might better explain the experimental results is one including CuL and CuL(OH)$_x$ species (x = 1 or 2). To adjust the experimental data, two models were tested: (i) Model I containing CuL and CuL(OH) species and (ii) Model II, where CuL, CuL(OH), and CuL(OH)$_2$ species were included. Optimization and refinement of the stability constants of the Cu-BES system were performed using the experimental and calculated complex formation curves. Table 5 shows, the refined stability constants for the DCP experiments. Both models fit rather well the experimental values, but model II was able to consistently fit the experimental data with a lower global standard deviation error, compared with model I, as seen in table 5. The differences between both models are small, although it is possible to see that, in model I, the refined stability constant values for CuL(OH) is higher than those refined by model II due to compensation of the absence of CuL(OH)$_2$ species. The final values, calculated from all the data collected by DCP and GEP, for the Cu-BES system are found in table 4.

In order to test the model, SDDs were drawn, using the values from tables 2 and 4, for GEP ($[L_T] : [Cu_T] = 4$, $[Cu_T] = 1 \times 10^{-3}$ M) [figure 4(C)] and DCP conditions ($[L_T] : [Cu_T] = 100$, $[Cu_T] = 3 \times 10^{-5}$ M) [figure 4(D)]. From analysis of the SDD [figures 4(C) and 4(D)], it is possible to see that complexation starts at pH 4.0. For the lower $[L_T] : [Cu_T]$ ratio [figure 4(C)], only at pH $\approx$ 4.5 is there enough complexed metal to be measureable (pL $\approx$ 5.5), as a CuL species. The Z_M function shows similar behavior as it starts to increase at pL = 5.5 [figure 3(C)]. For pH higher than 6.0, CuL(OH) is the major species in the system [figure 4(C)]. Again, this is in line with our observations of the Z_M function as it shows signs of back-fanning from pL = 4 to pL ~ 3 (pH 6 to pH ~6.5). Prior to precipitation (about pH 6.5), CuL(OH)$_2$ can be formed although at very low quantities, which explains why it is not possible to refine this species from GEP experiments. From SDD drawn for $[L_T] : [Cu_T] = 100$, $[Cu_T] = 3 \times 10^{-5}$ M [figure 4(D)], it is possible to see that both CuL(OH) and CuL(OH)$_2$ are present in good quantities in the pH range studied. This enabled determination of CuL(OH)$_2$ for DCP conditions unlike for GEP. In polarographic conditions, the precipitation is predicted by SDD to occur at pH 8, as seen in the intensity of the limiting current *versus* pH plot [figure 5(B)], a drop in intensity, characteristic of precipitation phenomena, is recorded at pH 8, which supports our model. In addition, the SDD for potentiometric conditions predicts precipitation at pH 6.5, which was recorded experimentally.

3.3. *Evaluation of complex stability constants and structures*

By comparing both ligands, it is possible to see clearly that BTP has stronger complexing capability with Cu than BES. This may be explained by the fact that BTP can form bidentate complexes, while BES cannot. To further support this claim, the comparison of the stability constant of NH_3 ($\log \beta_{Cu\text{-}NH3} = 4.08$ [19]) with those of BTP ($\log \beta_{Cu\text{-}BTp} = 10.7$) and BES ($\log \beta_{Cu\text{-}BES} = 3.24$) shows that BTP's constant is more than twice that of NH_3, while BES's constant is actually lower than that of NH_3. The structure of both ligands may also help to explain such differences. While BTP has two secondary amines, which allows it to act as a bidentate ligand, and BES has one tertiary amine, which only enables it to form one bond per ligand.

In the case of Cu-BTP, the values for CuL, CuL(OH), and CuL(OH)$_2$, described in the present study, are in agreement with those found by Hong and Bai [10]. If we compare the obtained constant values with the ones we would predict by adding the values of CuL$_X$ and

$Cu(OH)_X$ (theoretical values) for CuL(OH) [CuL(OH) = 19.4 *versus*. CuL(OH) = CuL + Cu (OH) = 10.73 + 6.10 = 16.83] and $CuL(OH)_2$ [$CuL(OH)_2$ = 24.3 *versus* $CuL(OH)_2$ = CuL + $Cu(OH)_2$ = 10.73 + 11.80 = 22.53], we can see that the obtained values are consistently larger that the theoretical values. If they would be similar, this could mean that a regular mechanism of water hydrolysis (from the coordination sphere) would take place [25]. Also, when we compare the constant values for CuL species of BTP and that of 1,3-diaminopropane (DP) (K_{CuL} = 9.7) [19], we can see that BTP has a larger stability constant for CuL even though the protonation constant of BTP is lower than that of DP (pK_{a1} = 10.54), which indicates possible coordination by other groups than the amines [10]. However, the differences found may be related with different mechanisms of CuL_x hydrolysis, as a proton may be also lost from the ligand itself, namely from the hydroxyl moieties [25]; thus, the larger values found may be related to the binding of the metal with the hydroxyl groups of BTP, which enlarges the stability constant values due to a chelating effect. Therefore, two possible pathways can be proposed to explain deprotonation of $CuL(OH)_x$ species (figure 6). Pathway 1 admits that both nitrogens and two oxygens from the terminal alcohol moieties would bind to the metal, and deprotonation would occur from these oxygens, while pathway 2 depicts CuL as being solely coordinated by nitrogens and, as each deprotonation occurs in the hydroxyl groups, oxygens bind to the metal ion.

To further explore this issue, UV–vis studies were conducted. The results from the UV–vis are presented in figure 7(A). All complexes have a λ_{max} between 600 and 630 nm and all the $CuL(OH)_x$ species have higher λ_{max} than $CuL_2(OH)_x$ species. As a first exercise, Prenesti's formula [26] used to estimate the λ_{max} for Cu(II) complexes as a function of coordinating groups was applied to the complexes expected in our system. The experimental λ_{max} obtained are close but consistently higher compared to the ones calculated by Prenesti's formula, in particular for $CuL_2(OH)_x$ species. This can be explained by the presence of axial coordination, which is known to cause a red shift on the λ_{max} for Cu(II) complexes [27, 28], namely a shift of about 50 nm (per each axial coordination), which was the shift

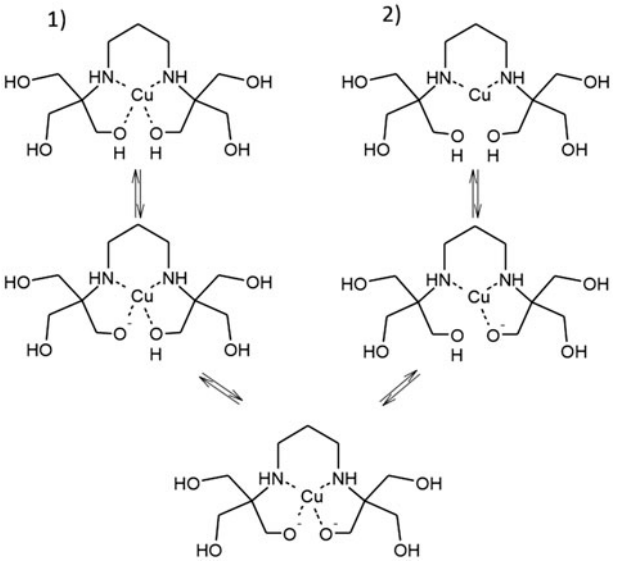

Figure 6. Proposed pathways for the coordination of BTP with Cu(II).

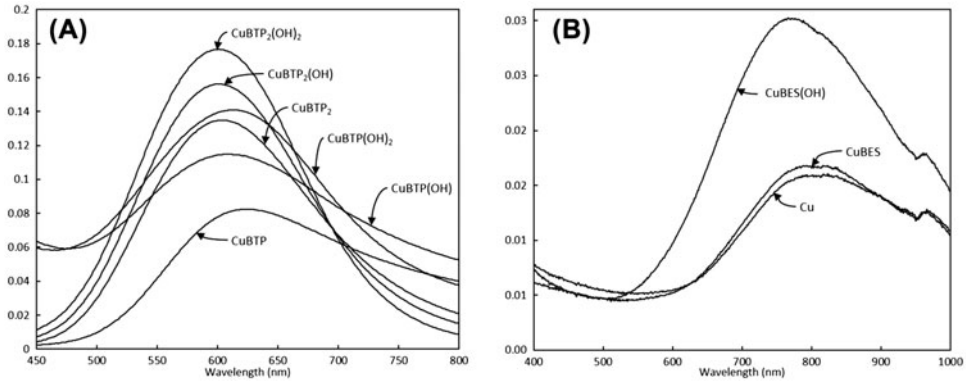

Figure 7. UV–vis spectroscopic data recorded for (**A**) Cu(II)-BTP system and for (**B**) Cu(II)-BES system with $[L_T] : [Cu_T] = 2$, $[Cu_T] = 1 \times 10^{-3}$ M. Species indicated represent the major species present in solution at sampled pH, with exception for Cu-BES and Cu-BES-OH, where the major species is always the free copper ion.

observed. On the other hand, given that these formulations are subject to some deviation [26], related to the structural variety, a likely reason for this deviation is structural. So, in the presence of complexes with coordination number of 4, where possible distortion phenomena cause a decrease in energy in the crystal-field splitting, result in a wavelength increase. Nevertheless, a pattern in both ratios may be deduced. In $[L_T] : [Cu_T] = 2$, CuL_2, $CuL_2(OH)$, and $CuL_2(OH)_2$ complexes have similar λ_{max} (604, 601, and 601, respectively). If the complex has four coordination spots, in $CuL_2(OH)_x$ species, all these spots would be occupied by the four nitrogens from two BTP molecules; therefore, no substantial shift in the λ_{max} should be observed, from one species to the other, which is observed in the data experimentally collected. Only CuL_2 presents a slightly higher λ_{max}, which may be related to a small quantity of CuL(OH) present in solution [figure 4(A)]. Therefore, axial coordination may be disregarded and the coordination by four nitrogens is held. On the other hand, for $[L_T] : [Cu_T] = 1.05$ it is possible to observe some differences between different species. The highest λ_{max} was found for CuL (624 nm), while both CuL(OH) and $CuL(OH)_2$ have lower λ_{max} (615 and 609 nm, respectively). The value for CuL can be explained by the presence of free Cu(II) in solution at the sampled pH [figure 4(B)], which is contributing to increasing λ_{max}, while CuL(OH) and $CuL(OH)_2$ both have high percentages in equilibrium [around 90%, figure 4(B)]; therefore, similar values were recorded. If one imagines a complex, where both nitrogens of the ligand are coordinating the metal together with a pair of oxygens, deprotonation may occur from the hydroxyl coordinating to the metal, as this makes them more susceptible to deprotonate [10], and the small differences on λ_{max} seen are related to different levels of deprotonation on coordinating oxygen [29]. Using the parameters described by Prenesti [26], if pathway 2 occurs, larger changes in λ_{max} would be expected and for CuL the λ_{max} value would be much higher.

Comparison of the stability constants of BTP with those of other ligands that have DP as root, such as N,N′-dimethylpropan-1,3-diamine (DPD), or 2-((3-aminopropyl)amino)ethanol (AAE), provides further evidence for pathway 1. While DPD has slightly higher pKa's ($pKa_1 = 8.81$ and $pKa_2 = 10.64$ [19]) than that of DP, and therefore its amines are more basic, the stability constant for Cu(II) ($K_{CuL} = 8.38$) [19] is lower than that of DP; so, the increase in side chains of DP do not increase the ability to bind copper in solution. On the other hand, AAE has a hydroxyl substituent with capability to bind to metal and its stability

constant for copper is two log units higher (K_{CuL} = 10.48) [19] than that of DPD, even though they have similar pKa's. Therefore, the resulting stability constants found for Cu(II)-BTP are supportive of proposed pathway 1.

For the Cu-BES system, the CuL stability constant value, already described in the literature [16], is slightly higher than the one found in this work. This may be related to possible compensation due to the fact that other species, such as CuL(OH), which should be present in significant quantities regardless of the ratio used, were not considered in the model. When comparing the obtained stability constant values with the theoretical ones for CuL(OH) [CuL(OH) = 10.9 *versus* CuL (OH) = CuL + Cu(OH) = 3.24 + 6.10 = 9.34] and CuL $(OH)_2$ [CuL$(OH)_2$ = 16.0 *versus* CuL$(OH)_2$ = CuL + Cu$(OH)_2$ = 3.24 + 11.80 = 15.04], a similar pattern to the Cu-BTP system can be found. However, the differences are much smaller than those found in the Cu-BTP system (only one log unit; whereas in the Cu-BTP system, differences of at least two log units were found). UV–vis studies were conducted to investigate this issue. Unfortunately, due to precipitation, only a very short pH range was available for analysis, in which the amounts of complex present were not high. However, the measured λ_{max} differ significantly (823, 802, and 766 nm for free copper ion, CuL, and CuL(OH), respectively, figure 7(B)), and a shift to blue wavelengths is found, consistent with the presence of complexation, as described by GEP and DCP. In fact, using Prenesti's method, and considering only one nitrogen bonded to Cu(II) and the relative percentages of each species predicted in the speciation distribution diagram (CuL and CuL(OH) for pH 5.6 and 6.1, respectively), the values 808 and 778 nm are found; these values are close to the ones observed experimentally. By comparing the deprotonation constant for BES with that of taurine (pK_a = 8.93) [19], we see that taurine is substantially more basic (about two log units higher) than BES. However, the stability constants for CuL for both ligands do not differ as much (3.24 for BES *versus* 3.56 [19]). This fact suggests that, despite the reduced basicity of BES, it is able to coordinate copper as well as taurine; therefore, the hydroxyl groups must positively affect the copper coordination, without, however, coordinating to the metal. A further illustration of this effect is present on a similar ligand, DIPSO (which differs from BES in length of the sulfonic acid chain by one carbon and in one extra hydroxyl in that same chain), which has a pKa (7.47 [17]) of the same order of magnitude of BES, but has a higher stability constant for Cu(II) (K_{CuL} = 4.2) [17].

A quick look of the structure of both ligands may give some possible explanations of such behavior. BTP is larger and has a larger carbon backbone than BES. Thus, in the case of the Cu-BTP system, the distance from the various possible coordination sites is large enough for the molecule to bend and to adapt to a multidentate structure. On the other hand, BES is more compact and small; thus, the distortions in the molecular bonds that would be required for it to adapt for a multidentate configuration can be too large.

With this work, we contributed to the understanding of the complexing behavior of Cu(II) with BTP, and BES thanks to a meticulous graphical analysis of the GEP, DCP, and UV–vis data fulfilling one of Good's requirements for a proper biological buffer. Following this premise, these new models should be taken in consideration when planning experiments, where these buffers are used with Cu(II).

Acknowledgements

This work was financed by FEDER funds through Programa Operacional Factores de Competitividade – COMPETE and by National Funds through FCT – Fundação para

a Ciência e a Tecnologia in the ambit of the project Pest-C/EQB/LA0006/2013. The authors thank Professor Ignacy Cukrowski from the University of Pretoria (South Africa) for polarographic modeling software (3D-CFC program) and Professor Carlos Gomes from the Faculty of Sciences/Porto University for the COPOTISY program.

References

[1] N.E. Good, G.D. Winget, W. Winter, T.N. Connolly, S. Izawa, R.M.M. Singh. *Biochemistry*, **5**, 467 (1966).
[2] N.E. Good, S. Izawa. *Methods Enzymol.*, **24**, 53 (1972).
[3] W.J. Ferguson, K.I. Braunschweiger, W.R. Braunschweiger, J.R. Smith, J.J. McCormick, C.C. Wasmann, N.P. Jarvis, D.H. Bell, N.E. Good. *Anal. Biochem.*, **104**, 300 (1980).
[4] C.P. Keller, E. Van Volkenburgh. *Plant Physiol.*, **110**, 1007 (1996).
[5] T. Meissner, F. Eisenbeiss, B. Jastorff. *J. Chromatogr. A*, **810**, 201 (1998).
[6] T.M. Pabst, G. Carta, N. Ramasubramanyan, A.K. Hunter, P. Mensah, M.E. Gustafson. *Biotechnol. Progr.*, **24**, 1096 (2008).
[7] S.C. Atkinson, C. Dogovski, J. Newman, R.C.J. Dobson, M.A. Perugini. *Acta Crystallogr. Sect. C: Cryst. Struct. Commun.*, **67**, 1537 (2011).
[8] T. Laureys, I.S.S. Pinto, C.V.M. Soares, H.B. Boppudi, H.M.V.M. Soares. *J. Chem. Eng. Data*, **57**, 87 (2012).
[9] C.M.H. Ferreira, I.S.S. Pinto, G.M.S. Alves, S.M. Sedeghi, H.M.V.M. Soares. *J. Coord. Chem.*, **67**, 3354 (2014).
[10] K.H. Hong, K.S. Bai. *Bull. Korean Chem. Soc.*, **19**, 197 (1998).
[11] Y. Fujita, T. Tokunaga, H. Kataoka. *Anal. Biochem.*, **409**, 46 (2011).
[12] Y. Ito, N. Satoh, T. Ishii, J. Kumakura, T. Hirano. *Clin. Chim. Acta*, **427**, 86 (2014).
[13] M.E. Mamprin, S. Petrocelli, E. Guibert, J. Rodríguez. *CryoLetters*, **29**, 121 (2008).
[14] G. Miszczuk, M.G. Mediavilla, M.D. Pizarro, C. Tiribelli, J. Rodríguez, M.E. Mamprin. *CryoLetters*, **33**, 75 (2012).
[15] H. Vogel, C. Gerlach, C. Richert. *Nucleosides Nucleotides Nucleic Acids*, **32**, 17 (2013).
[16] H.A. Azab, A.M. El-Nady. *Monatsh. Chem. Chem. Monthly*, **125**, 849 (1994).
[17] C.M.M. Machado, S. Scheerlinck, I. Cukrowski, H.M.V.M. Soares. *Anal. Chim. Acta*, **518**, 117 (2004).
[18] I. Zawisza, M. Rózga, J. Poznański, W. Bal. *J. Inorg. Biochem.*, **129**, 58 (2013).
[19] A.E. Martell, R.M. Smith. *NIST Standard Reference Database 46 (Version 8.0)*, US Department of Commerce, National Institute of Standards and Technology, Washington, DC (2004).
[20] C.M.M. Machado, I. Cukrowski, P. Gameiro, H.M.V.M. Soares. *Anal. Chim. Acta*, **493**, 105 (2003).
[21] P.M. May, K. Murray, D.R. Williams. *Talanta*, **35**, 825 (1988).
[22] A.J. Bard, L.R. Faulkner. *Electrochemical Methods: Fundamentals and Applications*, 2nd Edn, John Wiley & Sons, New York, NY (2000).
[23] I. Cukrowski. *Anal. Chim. Acta*, **336**, 23 (1996).
[24] C.M.M. Machado, I. Cukrowski, H.M.V.M. Soares. *Helv. Chim. Acta*, **86**, 3288 (2003).
[25] S. Canepari, V. Carunchio, P. Castellano, A. Messina. *Talanta*, **47**, 1077 (1998).
[26] E. Prenesti, P.G. Daniele, M. Prencipe, G. Ostacoli. *Polyhedron*, **18**, 3233 (1999).
[27] E. Prenesti, P.G. Daniele, S. Berto, S. Toso. *Polyhedron*, **25**, 2815 (2006).
[28] L. Lomozik, L. Bolewski, R. Dworczak. *J. Coord. Chem.*, **41**, 261 (1997).
[29] E. Prenesti, P.G. Daniele, S. Toso. *Anal. Chim. Acta*, **459**, 323 (2002).